Linearized Modeling of Integrated Electricity and District Heating Systems with VF-VT Strategy Based on McCormick Envelopes

Xueyong Tang
Power Grid Planning & Research Center
Guizhou Power Grid Co. , Ltd.
Guiyang, China

Xiaocong Sun
College of Electrical Engineering
Zhejiang University
Hangzhou, China
12010026@zju.edu.com

Xia Yan
Power Grid Planning & Research Center
Guizhou Power Grid Co. , Ltd.
Guiyang, China

Sheng Wang
College of Electrical Engineering
Zhejiang University
Hangzhou, China

Yu Zhang
Power Grid Planning & Research Center
Guizhou Power Grid Co. , Ltd.
Guiyang, China

Changzheng Shao, Yi Ding*
College of Electrical Engineering
Zhejiang University
Hangzhou, China
yiding@zju.edu.cn

***Abstract*—Combined harnessing of electrical and thermal energies has strengthened the interdependence between electricity and heating systems. It offers extra flexibility to system operation and improves energy efficiency. However, the nonlinearity in the coordinated operation of integrated electricity and district heating systems (IEDHS) brings about computational difficulties. This paper proposes a linearized modeling technique for the IEDHS which operates in variable flow rate and variable temperature (VF-VT) mode. Firstly, the district heating and electricity distribution network, as well as the key components such as combined heat and power (CHP) units are modeled. Then, the coordinated optimal operation (COO) of the IEDHS is formulated. Furthermore, the bilinear terms due to the VF-VT strategy are linearized based on McCormick Envelopes. In this way, the COO problem is reformulated into a standard quadratic programming problem, which can be well addressed by off-the-shelf solvers. Finally, the numeric results demonstrate the potential benefits of the proposed technique in terms of reducing system operation cost and wind curtailment.**

Keywords—linearization, coordinated optimal operation, McCormick Envelopes, integrated electricity and district heating system

I. INTRODUCTION

Renewable generations such as wind power have been developed prosperously worldwide in recent years [1]. However, large amounts of wind generations are curtailed in winter due to the lack of flexibility of combined heat and power (CHP) units in Northern China [2]. The electricity output of the CHP unit is strictly constrained by its heat output. In cold seasons, the heat demand has a tendency opposite to the electricity demand but consistent with wind generation during off-peak hours. Thus the electricity output of CHP units could cover most of the electricity demand, leading to high wind power curtailments [3].

Given the tight interdependence between electrical and thermal energies, the cooperation of electricity systems and heating systems can reduce the wind curtailment by sufficiently using the advantages of these two energy resources [4]. The concept of integrated electricity and district heating system (IEDHS) is therefore proposed. The coordinated operation of IEDHS has been well developed over the past few years. A combined heat and electricity dispatch was formulated in [5] to coordinate the operation of electricity system and district heating system. The deployment optimization of a CHP-dominated power system with wind power, pumped hydro storage, and electric boilers was explored in [6]. In the researches above, the network model of the heating system is neglected. The coordinated optimization model was established to minimize the pumping cost and heat loss cost in [7, 8]. Systematic modeling of combined electricity and heat networks considering hydraulic and thermal circuits has been illustrated in [9]. A uniform framework in the Laplace domain was proposed in [10] from an electrical-analog perspective.

In the researches above, the flow model of the heating system is simplified. The control of the primary district heating network (DHN) mainly depends on two kinds of parameters: supply temperature and flow rate. Most of the aforementioned studies specified one of the parameters, thus eliminating bilinear terms at the cost of giving up a large part of the feasible region. However, more and more district heating networks are transformed into variable temperature and variable flow rate (VF-VT) systems, which allows the IEDHS to operate more flexibly by controlling the two aforementioned parameters [11]. Therefore, fast and robust modeling and solution methodologies for IEDHS operation with VF-VT strategy are urgently required.

To address the research gaps, this paper proposes a linearized modeling technique for IEDHS which operates with the VF-VT strategy. The contribution is twofold:

(1) The coordinated optimal operation (COO) of the IEDHS is formulated. The model balances heat and electricity demands over 24 hours with various energy sources.

This research is supported by the Key Scientific and Technological Project of China Southern Power Grid 067600KK52190010: Research on Key Technologies of Regional Multi-Energy System Planning and Operation Based on Digital Twins.

(2) The bilinear constraints inheriting from the VF-VT strategy are linearized by McCormick Envelopes. In this way, the COO problem is reformulated into a standard quadratic programming problem.

The remainder of the paper is organized as follows. Section II describes the structure of IEDHS. The COO of the IEDHS is formulated in Section III. Section IV linearized the problem by using McCormick Envelopes. The manifold benefits of the proposed technique are illustrated by the case study in Sections V. Section VI concludes the paper.

II. Structure of IEDHS.

A. Basic Introduction to the IEDHS

The IEDHS is comprised of a heating system and an electricity system. The heat sources in a heating system usually include CHP units, heat pumps, and electric boilers. They output thermal energy by heat media such as hot water or steam and then deliver the heat power to the customers through the DHN. The DHN consists of symmetric supply pipes and return pipes. The mass flow rates in the supply pipes are equivalent to those in the return pipes. If the mass flow rate is negative, that means the direction of the flow is opposite to the prescribed positive direction. At each source/load node, heat power is injected into/withdrawn from the network via a heat exchanger, as shown in Fig.1.

The operating strategy can be divided into the following four categories [12]: constant flow rate and constant temperature (CF-CT), variable flow rate and constant temperature (VF-CT), constant flow rate and variable temperature (CF-VT), and VF-VT. The CF-CT with maximum temperature and maximum flow rate is only adopted when the maximum heat demand is encountered. The VF-CT and CF-VT usually set either flow rate or temperature constant, thus the bilinear terms inheriting from the products of flow rates and temperatures are automatically avoided. However, a large part of the feasible region is given up. The VF-VT strategy entails adjusting flow rate and supply temperature simultaneously with respect to the variation of heat demand. It makes the system operation more energy efficient. In this paper, it is assumed that the DHN is operated with the VF-VT strategy.

Generally, the generating units in the IEDHS can be divided into electricity-only units, coupling devices, and heat-only units. In this paper, the electricity-only units include gas turbines (GT) and distributed wind generators (WG). The coupling devices include CHP units and electric boilers (EB). The heat-only units include gas-fired boilers (GB).

B. Heating System Model

A heating system consists of heat sources and a DHN. The DHN model characterizes the thermal and hydraulic conditions. Thermal conditions characterize the relations between nodal temperatures and heat demand/supply, which are explicated as follows:

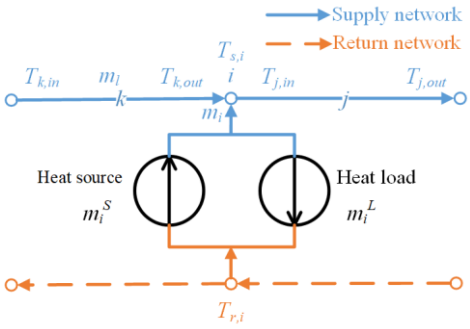

Fig. 1. General structure of a DHN node.

1) Heat demand/supply:

$$\Phi_i = cm_i(T_{s,i} - T_{r,i}) \tag{1}$$

where Φ_i is the heat demand/supply at heat load/source node i. c is the specific heat capacity of water. m_i is the mass flow rate in the pipe connecting the supply and return networks. $T_{s,i}$ and $T_{r,i}$ are the temperatures at the supply side and return side, respectively. $T_{s,i} > T_{r,i}$ always holds.

2) Fluid heat loss: Taking the heat loss into account, the temperature of the fluid in pipes drops along the flow directions. The relation between inlet and outlet temperatures of each pipe can be formulated as:

$$T_{out} = (T_{in} - T_{am})\mathrm{e}^{-\frac{\lambda L}{cm_l}} + T_{am} \tag{2}$$

where T_{in} and T_{out} are the inlet and outlet temperatures of the pipe, respectively. T_{am} is the ambient temperature. λ is the heat transfer coefficient of the pipe per unit length. L is the length of the pipe. m_l is the mass flow rate in the pipe.

3) Temperatures at confluence nodes: According to the energy conservation law, when fluids with different temperatures come across at a confluence node, the temperature of the mixture is calculated as:

$$(\sum m_l^k)T_{k,out} = \sum (m_l^k T_{j,in}), \forall k \in S_i^{pipe-}, \forall j \in S_i^{pipe+} \tag{3}$$

where S_i^{pipe-} and S_i^{pipe+} are the set of pipes whose outlet and inlet are connected to node i, respectively. m_l^k is the mass flow rate in pipe k. $T_{k,out}$ is the temperature at the outlet of pipe k. $T_{j,in}$ is the temperature at the inlet of pipe j.

Hydraulic conditions describe the mass flow and fluid pressure in pipes, including the following formula:

4) Fluid pressure loss: Due to the friction of pipes, the fluid pressure decreases along the pipe. The pressure loss is expressed as follows based on the Darcy-Weisbach equation [13]:

$$P_l = \frac{128L\mu}{\pi D^4} m_l \tag{4}$$

where P_l is the pressure loss along the pipe. μ is the fluid kinematic viscosity. D is the inner diameter of the pipe.

5) Continuity of mass flow: According to the mass conservation law, the mass flowing into a node is equal to the mass flowing out of the node.

$$\mathbf{A} \cdot m_l = m_i^S - m_i^L \tag{5}$$

where m_i^S and m_i^L are the mass flow rates of the heat sources and loads, respectively. The incidence matrix $\mathbf{A} = [a_{ik}]$ is defined as:

$$a_{ik} = \begin{cases} +1, k \in S_i^{pipe-} \\ 0, k \notin S_i^{pipe-} \bigcup S_i^{pipe+} \\ -1, k \in S_i^{pipe+} \end{cases} \tag{6}$$

6) Fluid pressure balance: According to the principle of pressure balance, the pressure loss in a closed loop is equal to zero.

$$\mathbf{B}_f \cdot P_l = 0 \tag{7}$$

where $\mathbf{B}_f$ is the basic loop matrix and can be defined as $\mathbf{B}_f = [b_{hk}]$. $b_{hk} = 1$ indicates that the direction of mass flow in pipe k is consistent with the direction of loop h; $b_{hk} = -1$ indicates that the direction of mass flow in pipe k is opposite to the direction of loop h.

It should be noticed that the flows in the DHN are maintained by a circulating water pump. Given it consumes little electricity, the cost of the circulating water pump is negligible in the DHN [14].

7) Heat sources: Three kinds of heat sources are considered: CHP units, EBs, and GBs.

The electricity output of a CHP unit is limited by its heat demand. The feasible operation region of an extraction-condensing CHP unit is shown in Fig. 2 [15].

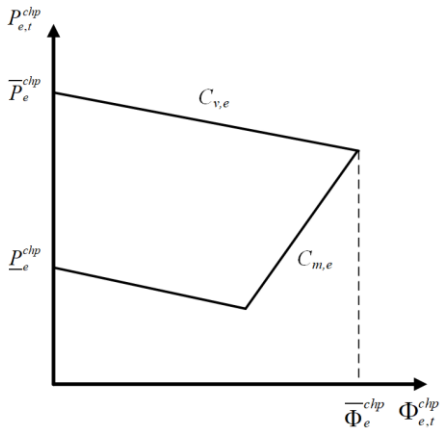

Fig. 2. The feasible region of heat and electricity outputs in the CHP unit.

$$\begin{aligned} \underline{P}_e^{chp} - c_{v,e}\Phi_{e,t}^{chp} \le P_{e,t}^{chp} \le \overline{P}_e^{chp} - c_{v,e}\Phi_{e,t}^{chp} \\ 0 \le \Phi_{e,t}^{chp} \le \left(P_{e,t}^{chp} - \overline{P}_e^{chp} + (c_{v,e} + c_{m,e})\overline{\Phi}_e^{chp} \right) / c_{m,e} \end{aligned} \tag{8}$$

where e is the index of CHP units. $c_{m,e}$ is the heat-to-electricity ratio of the CHP unit operating at back pressure. $c_{v,e}$ is the electricity output reduction of the CHP unit operating at extraction-condensing to produce heat. $\overline{P}_e^{chp}$ and $\underline{P}_e^{chp}$ are the maximum and minimum electricity output of the CHP unit, respectively. $\overline{\Phi}_e^{chp}$ is the maximum heat output of the CHP unit. $P_{e,t}^{chp}$ and $\Phi_{e,t}^{chp}$ are the electricity and heat output of the CHP unit, respectively.

The operation cost of CHP units is a bi-variate convex quadratic function with respect to their electricity and heat outputs.

$$C_t^{chp} = \sum_e \left(a_e^2 (P_{e,t}^{chp} + c_{v,e}\Phi_{e,t}^{chp})^2 + a_e^1 (P_{e,t}^{chp} + c_{v,e}\Phi_{e,t}^{chp}) + a_e^0 \right) \tag{9}$$

where a_e^m is the m^{th} cost coefficient of the CHP unit.

EBs convert electricity into heat, outputting a certain amount of heat steam, water, or other thermal media. The operation cost of EBs is formulated as:

$$C_t^{eb} = \sum_f \Gamma \frac{\Phi_{f,t}^{eb}}{\eta_f} \tag{10}$$

where f is the index of EBs. $\Phi_{f,t}^{eb}$ is the heat output of the EB. η_f is the efficiency of the EB. Γ is the electricity price.

The operation cost of a GB is defined as a quadratic function of the heat output [5].

$$C_t^{gb} = \sum_g \left(b_g^2 (\Phi_{g,t}^{gb})^2 + b_g^1 \Phi_{g,t}^{gb} + b_g^0 \right) \tag{11}$$

where g is the index of GBs. $\Phi_{g,t}^{gb}$ is the heat output of the GB. b_g^m is the m^{th} cost coefficient of the GB.

C. Electricity System Model

1) Linearized branch flow model: Considering the distribution network usually has a radial topology structure, the model of the electricity network can be described by the linearized branch flow model [16]. The typical topology is shown in Fig. 3.

$$P_{ij} + \sum_j P_j^g == \sum_{k \in \pi(j)} P_{jk} + \sum_j P_j^d \tag{12}$$

$$Q_{ij} + \sum_j Q_j^g = \sum_{k \in \pi(j)} Q_{jk} + \sum_j Q_j^d \tag{13}$$

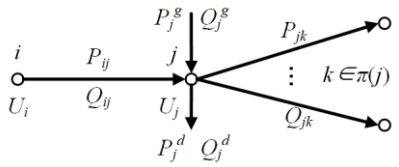

Fig. 3. Typical topology of the linearized branch flow model.

$$U_j = U_i - \frac{r_{ij}P_{ij} + x_{ij}Q_{ij}}{U_0} \tag{14}$$

where P_{ij} and Q_{ij} are active power and reactive power in distribution line *ij*. P_j^g and Q_j^g are active and reactive power generations at bus *j*. P_j^d and Q_j^d are active and reactive power demands at bus *j*. r_{ij} and x_{ij} are line resistance and reactance. U_j and U_0 are voltage magnitude at bus *j* and slack bus, respectively. $\pi(j)$ is the set of nodes whose injection power is flowing from node *j* .

2) Electricity generation model: In this paper, three kinds of electricity sources are considered including GTs, distributed WGs, and CHP units. CHP units have already been modeled in section II-A.

The operation cost of GTs is defined as a quadratic function of the electricity output [14].

$$C_h^{gt} = \sum_h \left(c_h^2 (P_{h,t}^{gt})^2 + c_h^1 P_{h,t}^{gt} + c_h^0 \right) \tag{15}$$

where *h* is the index of GTs. $P_{h,t}^{gt}$ is the electricity output of the GT unit. c_h^m is the m^{th} cost coefficient of the GT unit.

The penalty cost of distributed WGs is proportional to wind power curtailment.

$$C_t^{wind} = \sigma \sum_n \left(\overline{Wg}_{n,t} - Wg_{n,t} \right) \tag{16}$$

where *n* is the index of distributed WGs. $Wg_{n,t}$ and $\overline{Wg}_{n,t}$ is the real electricity output and predicted available generating capacity of the distributed WG. σ is the penalty factor of wind curtailment.

III. Formulation of COO

In this section, the COO problem is formulated. The proposed COO seeks the optimal operating point of electricity generation units and heat sources to minimize the operation cost.

In the COO model, the decision variables regarding the electricity system include: the electricity output of GTs (P_h^{gt}), distributed WGs (Wg_n), and CHP units (P_e^{chp}) as well as the electricity demand of EBs (Pd_f^{eb}). The decisions regarding the heating system include: the heat output of CHP units (Φ_e^{chp}), EBs (Φ_f^{eb}), and GBs (Φ_g^{gb}); mass flow rates in water pipes (m_l), sources (m_i^S), and loads (m_i^L); temperatures of nodes at the supply side ($T_{s,i}$) and return side ($T_{r,i}$), inlet temperatures (T_{in}), and outlet temperatures (T_{out}).

The objective is to minimize the total operation cost.

$$Min\left\{ \sum_{t=1}^{24} \left(C_t^{chp} + C_t^{eb} + C_t^{gb} + C_t^{gt} + C_t^{wind} \right) \right\} \tag{17}$$

where $C_t^{chp}, C_t^{eb}, C_t^{gb}, C_t^{gt}$ and C_t^{wind} are defined in (9), (10), (11), (15), and (16), respectively.

Subject to:

1) Mass flow rate limits: Mass flow rates in pipes should be constrained within their limits.

$$\begin{aligned} \underline{m_l} \le m_l \le \overline{m_l} \\ \underline{m_i} \le m_i \le \overline{m_i} \end{aligned} \tag{18}$$

2) Temperature limits: The temperatures should be constrained within their limits.

$$\underline{T_{s,i}} \le T_{s,i} \le \overline{T_{s,i}}, \underline{T_{r,i}} \le T_{r,i} \le \overline{T_{r,i}} \tag{19}$$

$$\underline{T_{in}} \le T_{in} \le \overline{T_{in}}, \underline{T_{out}} \le T_{out} \le \overline{T_{out}} \tag{20}$$

3) Electricity output constraints of GTs: The Electricity outputs of GTs are within their technical limits.

$$\underline{P_h^{gt}} \le P_{h,t}^{gt} \le \overline{P}_h^{gt} \tag{21}$$

4) Electricity output constraints of distributed WGs: The electricity outputs of the distributed WGs are limited by their available wind power.

$$0 \le Wg_{n,t} \le \overline{Wg}_{n,t} \tag{22}$$

5) Heat output constraints of EBs: The heat outputs of EBs are constrained by their limits.

$$0 \le \Phi_{f,t}^{eb} \le \overline{\Phi}_f^{eb} \tag{23}$$

6) Heat output constraints of GBs: The heat outputs of GBs are constrained by their limits.

$$0 \le \Phi_{g,t}^{gb} \le \overline{\Phi}_g^{gb} \tag{24}$$

7) CHP units constraints (8)
8) Electricity network constraints (12)-(14)
9) Heat demand/supply constraints (1)
10) Fluid heat loss constraints (2)
11) Constraints of temperatures at confluence nodes (3)
12) Fluid pressure loss constraints (4)
13) Continuity of mass flow constraint (5)
14) Fluid pressure balance constraints (7)

IV. A Linearization Approach Based on McCormick Envelopes

Observing the COO problem, all the operation costs in the objective function are quadratic. However, the constraints are nonlinear due to products of mass flow rates and temperatures in constraints (1), (3), and exponential functions in constraints (2).

According to (2), the heat power loss along the pipe is defined as:

$$\Phi_l = cm_l(T_{in} - T_{out}) = cm_l(T_{in} - T_{am})(1 - e^{-\frac{\lambda L}{cm_l}}) \quad (25)$$

In practice, $0 < \lambda L / cm_l \ll 1$. Using the equivalent infinitesimal $e^{-x} = 1 - x$, (25) can be approximated as [17]:

$$\Phi_l \approx cm_l(T_{in} - T_{am})\frac{\lambda L}{cm_l} = \lambda L(T_{in} - T_{am}) \quad (26)$$

From the equation above, we can see that the heat power loss only depends on the inlet temperatures of pipes. This means that for a pipe with certain length and heat transfer coefficient, the lower the inlet temperature is, the lower the heat power loss is.

The constraints of heat demand/supply (1) and temperature at confluence nodes (3) both have bilinear terms inheriting from the VF-VT strategy. In this paper, we use McCormick Envelopes to guarantee convexity and keep the bounds sufficiently tight [18].

By adopting McCormick Envelopes, (1) can be replaced by (27).

$$\begin{aligned}
&\Phi_i = c(w_{s,i} - w_{r,i}) \\
&w_{s,i} \ge \underline{m_i}T_{s,i} + m_i\underline{T_{s,i}} - \underline{m_i}\underline{T_{s,i}} \\
&w_{s,i} \ge \overline{m_i}T_{s,i} + m_i\overline{T_{s,i}} - \overline{m_i}\overline{T_{s,i}} \\
&w_{s,i} \le \overline{m_i}T_{s,i} + m_i\underline{T_{s,i}} - \overline{m_i}\underline{T_{s,i}} \\
&w_{s,i} \le m_i\overline{T_{s,i}} + \underline{m_i}T_{s,i} - \underline{m_i}\overline{T_{s,i}} \\
&w_{r,i} \ge \underline{m_i}T_{r,i} + m_i\underline{T_{r,i}} - \underline{m_i}\underline{T_{r,i}} \\
&w_{r,i} \ge \overline{m_i}T_{r,i} + m_i\overline{T_{r,i}} - \overline{m_i}\overline{T_{r,i}} \\
&w_{r,i} \le \overline{m_i}T_{r,i} + m_i\underline{T_{r,i}} - \overline{m_i}\underline{T_{r,i}} \\
&w_{r,i} \le m_i\overline{T_{r,i}} + \underline{m_i}T_{r,i} - \underline{m_i}\overline{T_{r,i}} \\
&\underline{m_i} \le m_i \le \overline{m_i} \\
&\underline{T_{s,i}} \le T_{s,i} \le \overline{T_{s,i}}, \underline{T_{r,i}} \le T_{r,i} \le \overline{T_{r,i}}
\end{aligned} \quad (27)$$

Similarly, (3) can be transformed into a linearized model by adopting McCormick Envelopes.

In this way, the COO problem is reformulated into a standard quadratic programming problem. In this paper, the optimization model is solved using YALMIP [19] by calling CPLEX [20].

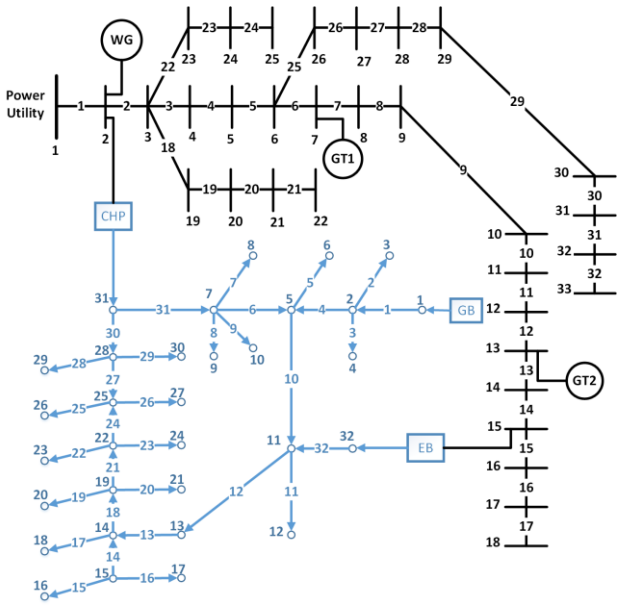

Fig. 4. Topology of the IEDHS.

V. Case Studies

A. System Configurations

A test IEDHS is used to validate the proposed method. The test system is composed of an IEEE 33-bus electricity network and a 32-node DHN modified from [9, 21], as shown in Fig. 4. The electricity-only units include two GTs and a distributed WG. The coupling devices consist of a CHP unit and an EB. The heat-only unit refers to the GB. Static var generators with the capacity of 1.5 and 2.0 MVar are located at bus 3 and bus 12 for compensating reactive power and maintaining the voltage, respectively. Parameters of the CHP unit, distributed WG, GB, GTs, EB, and the boundaries of control variables are listed in Table I.

The profiles of the hourly electricity demand, heat demand, and forecasted maximum wind generation are shown in Fig. 5. The electricity and heat demand profiles are derived from [21].

The proposed model is applied to the test system over 24 hours. All simulations are conducted on a laptop with Intel i7-6700HQ CPU and 8G memory. The simulation results from two scenarios are compared.

Case 1: the DHN is controlled by the CF-VT strategy.

Case 2: the DHN is controlled by the VF-VT strategy.

TABLE I. Parameters of IEDHS

Variable	Value	Variable	Value
$a_e^2 / a_e^1 / a_e^0$	0.37/26.98/41.53	η_f / σ	0.9/20
$b_g^2 / b_g^1 / b_g^0$	0.15/20/40	$\underline{T_{s,i}} / \overline{T_{s,i}}$	70/100
$c_{h_1}^2 / c_{h_1}^1 / c_{h_1}^0$	0.12/20/50	$\underline{T_{r,i}} / \overline{T_{r,i}}$	35/70
$c_{h_2}^2 / c_{h_2}^1 / c_{h_2}^0$	0.09/15/55	$\underline{m_l} / \overline{m_l}$	-15/15
$c_{v,e} / c_{m,e}$	0.15/0.55	$\underline{m_i} / \overline{m_i}$	-15/15

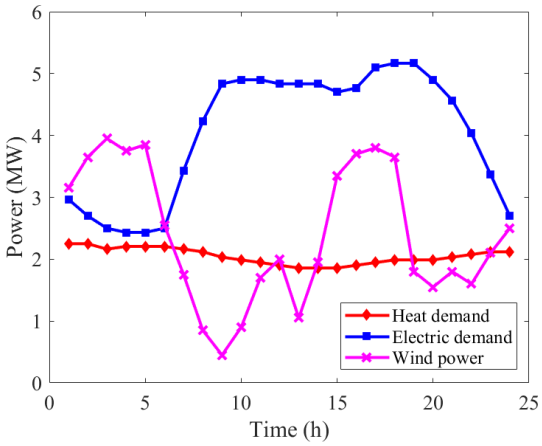

Fig. 5. Electricity demand, heat demand, and wind power generation profiles.

B. Analysis of the Simulation Results

1) Operation costs and wind power accommodation

In Case 1, mass flow rates are specified according to [21]. The operation costs and wind penalty costs are shown in Table II. We can see that the operation cost and wind penalty cost in Case 2 is much lower than those in Case 1. Compared with Case 1, the IEDHS in Case 2 can save the operation cost by 216.9 $ and wind penalty cost by 86.23 $ in a typical day, respectively. The results interpret that the VF-VT strategy can remarkably reduce the operation cost, and in the meantime accommodate the wind power well.

The wind power accommodation ratio in Case 1 and Case 2 are compared in Fig. 6. As we can see, wind power curtailment only occurs during the off-peak hours. We can also observe that wind power curtailment can be reduced significantly in Case 2. In Case 2, the DHN operator can regulate flow and supply temperature simultaneously with respect to the variation of heat demand, thus expanding the feasible region and achieving a better optimal solution than Case 1. Thereby, the wind power can be utilized effectively.

TABLE II. OPERATION COST AND WIND PENALTY COST

	Operation Cost ($)	Wind Penalty Cost ($)
Case 1	4137.1	123.0627
Case 2	3920.2	36.7937

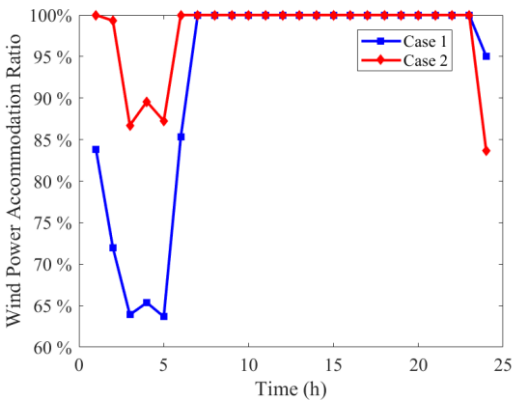

Fig. 6. Wind power accommodation ratio in two cases.

2) Mass flow rates and Temperatures

The mass flow rates of pipes and the nodal temperatures at the supply side and return side in Case 1 and Case 2 are shown in Fig. 7 and Fig. 8, respectively. We can see that for a certain heat demand, the difference between the supply and return temperatures is higher with smaller water flow. Given the specified mass flow rate with CF-VT strategy, the temperature can only be adjusted in a very small range. However, the VF-VT strategy can adjust the mass flow rate and temperature flexibly in a greater scope.

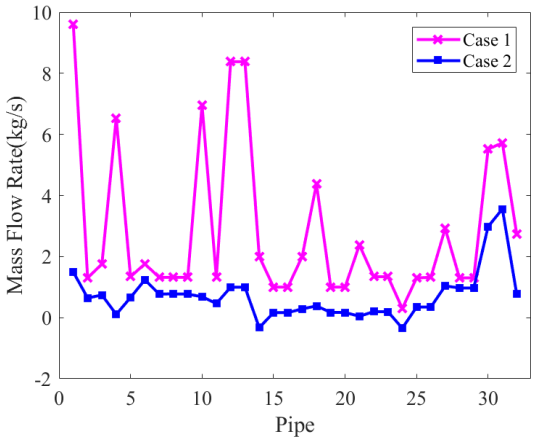

Fig. 7. Mass flow rates in two cases.

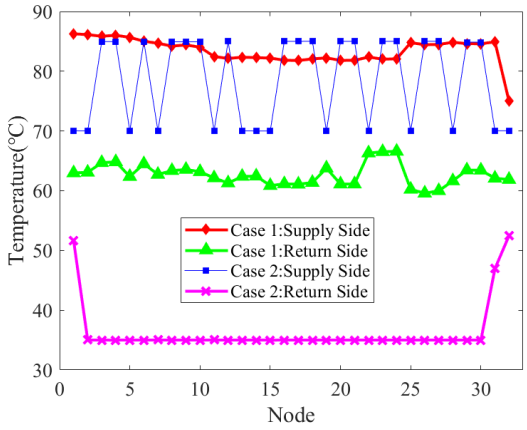

Fig. 8. Nodal temperatures in two cases.

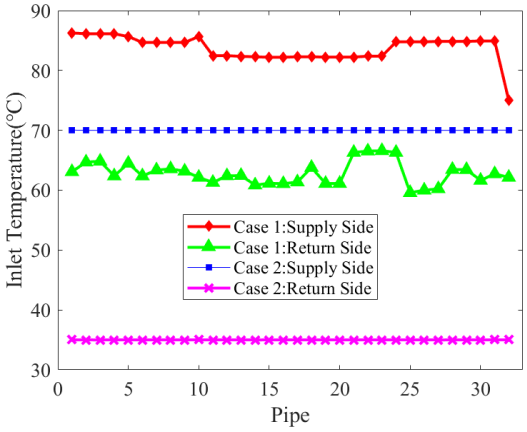

Fig. 9. Inlet temperatures of pipes in two cases.

The inlet temperatures of pipes in Case 1 and Case 2 are shown in Fig. 9. According to (26), the heat power loss only depends on the inlet temperatures of pipes. As

we can see, the inlet temperatures of pipes in Case 2 are lower than those in Case 1. This verifies that the power loss of the system with the VF-VT strategy is much lower than that with the CF-VT strategy.

VI. Conclusions

In this paper, a linearized modeling technique for the IEDHS which operates in VF-VT mode is proposed. The COO of IEDHS is formulated. The bilinear constraints due to the VF-VT strategy are linearized based on McCormick Envelopes. In this way, the COO problem is reformulated into a standard quadratic programming problem. The proposed technique is used in a modified testing system, we find that the IEDHS with the VF-VT strategy is more energy efficient and cost effective in daily operation. Compared with the CF-VT strategy, the IEDHS with the VF-VT strategy can reduce the operation cost by 216.9 $, and the wind penalty cost by 86.23 $ in a typical day, respectively. The proposed technique can improve the computational efficiency of IEDHS with VF-VT strategy, and contribute to the day-ahead unit commitment in IEDHS as well.

Acknowledgment

The research is supported by the Key Scientific and Technological Project of China Southern Power Grid 067600KK52190010: Research on Key Technologies of Regional Multi-Energy System Planning and Operation Based on Digital Twins.

References

[1] X. Yang, Y. Song, G. Wang, and W. Wang, "A comprehensive review on the development of sustainable energy strategy and implementation in China," *IEEE Transactions on Sustainable Energy*, vol. 1, no. 2, pp. 57-65, 2010.

[2] X. Chen, M. B. McElroy, and C. Kang, "Integrated Energy Systems for Higher Wind Penetration in China: Formulation, Implementation and Impacts," *IEEE Transactions on Power Systems*, pp. 1-1, 2017.

[3] X. Chen, C. Kang, M. O'Malley, Q. Xia, J. Bai *et al.*, "Increasing the Flexibility of Combined Heat and Power for Wind Power Integration in China: Modeling and Implications," *IEEE Transactions on Power Systems*, vol. 30, no. 4, pp. 1848-1857, JULY 2015.

[4] H. Chen, T. Zhang, R. Zhang, T. Jiang, X. Li *et al.*, "Interval optimal scheduling of integrated electricity and district heating systems considering dynamic characteristics of heating network," *IET Energy Systems Integration*, 2020.

[5] Z. Li, W. Wu, M. Shahidehpour, J. Wang, and B. Zhang, "Combined Heat and Power Dispatch Considering Pipeline Energy Storage of District Heating Network," *IEEE Transactions on Sustainable Energy*, vol. 7, no. 1, pp. 12-22, 2016.

[6] N. Zhang, X. Lu, M. B. McElroy, C. P. Nielsen, X. Chen *et al.*, "Reducing curtailment of wind electricity in China by employing electric boilers for heat and pumped hydro for energy storage," *Applied Energy*, vol. 184, pp. 987-994, 2016.

[7] E. Guelpa, C. Toro, A. Sciacovelli, R. Melli, E. Sciubba *et al.*, "Optimal operation of large district heating networks through fast fluid-dynamic simulation," *Energy*, vol. 102, pp. 586-595, 2016.

[8] P. Jie, N. Zhu, and D. Li, "Operation optimization of existing district heating systems," *Applied Thermal Engineering*, vol. 78, pp. 278-288, 2015.

[9] X. Liu, J. Wu, N. Jenkins, and A. Bagdanavicius, "Combined analysis of electricity and heat networks," *Applied Energy*, vol. 162, pp. 1238-1250, 2016.

[10] J. Yang, N. Zhang, A. Botterud, and C. Kang, "On An Equivalent Representation of the Dynamics in District Heating Networks for Combined Electricity-Heat Operation," *IEEE Transactions on Power Systems*, vol. 35, no. 1, pp. 560-570, 2020.

[11] J. Duquette, A. Rowe, and P. Wild, "Thermal performance of a steady state physical pipe model for simulating district heating grids with variable flow," *Applied Energy*, vol. 178, pp. 383-393, 2016.

[12] M. Pirouti, "Modelling and analysis of a district heating network," Cardiff University, 2013.

[13] G. O. Brown, "The history of the Darcy-Weisbach equation for pipe flow resistance," in *Environmental and Water Resources History*, 2003, pp. 34-43.

[14] Y. Cao, W. Wei, L. Wu, S. Mei, M. Shahidehpour *et al.*, "Decentralized Operation of Interdependent Power Distribution Network and District Heating Network: A Market-Driven Approach," *IEEE Transactions on Smart Grid*, vol. 10, no. 5, pp. 5374-5385, 2019.

[15] M. Kia, M. Setayesh Nazar, M. S. Sepasian, A. Heidari, and P. Siano, "An efficient linear model for optimal day ahead scheduling of CHP units in active distribution networks considering load commitment programs," *Energy*, vol. 139, pp. 798-817, 2017.

[16] H.-G. Yeh, D. F. Gayme, and S. H. Low, "Adaptive VAR Control for Distribution Circuits With Photovoltaic Generators," *IEEE Transactions on Power Systems*, vol. 27, no. 3, pp. 1656-1663, 2012.

[17] C. Shao, Y. Ding, J. Wang, and Y. Song, "Modeling and Integration of Flexible Demand in Heat and Electricity Integrated Energy System," *IEEE Transactions on Sustainable Energy*, vol. 9, no. 1, pp. 361-370, 2018.

[18] M. Bynum, A. Castillo, J.-P. Watson, and C. D. Laird, "Tightening McCormick Relaxations Toward Global Solution of the ACOPF Problem," *IEEE Transactions on Power Systems*, vol. 34, no. 1, pp. 814-817, 2019.

[19] J. Lofberg, "YALMIP : a toolbox for modeling and optimization in MATLAB," in *IEEE International Symposium on Computer Aided Control Systems Design*, 2005, pp. 284-289.

[20] I. I. Cplex, "V12. 1: User's Manual for CPLEX," *International Business Machines Corporation*, vol. 46, no. 53, p. 157, 2009.

[21] R. Li, W. Wei, S. Mei, Q. Hu, and Q. Wu, "Participation of an Energy Hub in Electricity and Heat Distribution Markets: An MPEC Approach," *IEEE Transactions on Smart Grid*, vol. 10, no. 4, pp. 3641-3653, 2019.